Microchimica Acta (2021) 188: 374
https://doi.org/10.1007/s00604-021-05006-6

ORIGINAL PAPER

Covalently modified enzymatic 3D-printed bioelectrode

Lujun Wang [1,2,3] · Martin Pumera [1,3,4,5]

Received: 2 June 2021 / Accepted: 25 August 2021 / Published online: 10 October 2021

Abstract

Three-dimensional (3D) printing has showed great potential for the construction of electrochemical sensor devices. However, reported 3D-printed biosensors are usually constructed by physical adsorption and needed immobilizing reagents on the surface of functional materials. To construct the 3D-printed biosensors, the simple modification of the 3D-printed device by non-expert is mandatory to take advantage of the remote, distributed 3D printing manufacturing. Here, a 3D-printed electrode was prepared by fused deposition modeling (FDM) 3D printing technique and activated by chemical and electrochemical methods. A glucose oxidase-based 3D-printed nanocarbon electrode was prepared by covalent linkage method to an enzyme on the surface of the 3D-printed electrode to enable biosensing. X-ray photoelectron spectroscopy and scanning electron microscopy were used to characterize the glucose oxidase-based biosensor. Direct electrochemistry glucose oxidase-based biosensor with higher stability was then chosen to detect the two biomarkers, hydrogen peroxide and glucose by chronoamperometry. The prepared glucose oxidase-based biosensor was further used for the detection of glucose in samples of apple cider. The covalently linked glucose oxidase 3D-printed nanocarbon electrode as a biosensor showed excellent stability. This work can open new doors for the covalent modification of 3D-printed electrodes in other electrochemistry fields such as biosensors, energy, and biocatalysis.

Keywords 3D-printed electrode · Electrochemical detection · Covalent modification · Hydrogen peroxide · Glucose

Introduction

Three-dimensional (3D) printing, also known as "additive manufacturing," is booming as an advanced manufacturing method for the fabrication of devices in various areas, such as medicine, biotechnology, electronics, engineering, and chemistry [1–3]. For the special area of electrochemistry, 3D printing has attracted great attention in energy storage, energy conversion, batteries, sensors, *etc*. [4, 5]. 3D printing techniques in electrochemistry mainly focus on the construction of desired electrodes and devices with merits of low-cost, fast prototyping and fabrication, and minimal waste [6–8]. Nowadays, various techniques have emerged to manufacture these electrochemical parts, including fused deposition modeling (FDM), inkjet printing, select laser melting (SLM), and stereolithography (SLA) [9–11]. Among these techniques, FDM is considered the most common method for the manufacture of desired electrodes [12, 13].

Materials for FDM 3D printing are usually constituted by thermoplastic materials, typically as polylactic acid (PLA) or acrylonitrile butadiene styrene (ABS), with other conducting materials such as graphene or carbon black [14–17]. Among them, a commercial graphene/PLA filament called "nanocarbon" using for printing 3D electrodes has become extremely popular in the academic research realm due to the low-cost materials and printers, which shows a great potential for replacement of the conventional electrodes [18, 19]. However, these as-printed electrodes are usually covered by large amounts of insulating materials; thus, a pre-treatment method is needed to remove these

This article is part of the Topical Collection on *3D printing manufacturing technologies for the advancement of analytical sciences*

✉ Martin Pumera
pumera.research@gmail.com

[1] Future Energy and Innovation Laboratory, Central European Institute of Technology, Brno University of Technology (CEITEC-BUT), 61200 Brno, Czech Republic

[2] School of Pharmacy, Southwest Medical University, Luzhou, Sichuan 646000, People's Republic of China

[3] 3D Printing and Innovation Hub, Department of Food Technology, Mendel University in Brno, Zemedelska 1, CZ-613 00 Brno, Czech Republic

[4] Department of Chemical and Biomolecular Engineering, Yonsei University, 50 Yonsei-ro, Seodaemungu, Seoul 03722, South Korea

[5] Department of Medical Research, China Medical University Hospital, China Medical University, No. 91 Hsueh-Shih Road, Taichung, Taiwan

non-conductive materials and expose the conductive sites. Many activated techniques have been reported to improve the electrochemical performance of these as-printed electrodes. Chemical activation using solvents is one of the common strategies to remove surface PLA [20–23]. Previously, our group first demonstrated that as-printed 3D nanocarbon electrodes can be activated by simply dimethylformamide (DMF) immersion, which can remove large amounts of PLA from the electrode's surface [13]. Then, our group demonstrated that the combination of DMF and electrochemical activation methods can further improve the activity of 3D-printed electrodes than DMF activation alone [24]. Mechanical polishing can also remove excess PLA and expose the conductive graphene materials [25, 26]. Other methods, such as proteinase digestion and sodium borohydride reduction, can also be used to improve the electrochemical activity of 3D-printed nanocarbon electrodes [27].

Besides the activation procedure for nanocarbon electrode described above, post-modification is considered as an important way to expand the application range of activated electrodes. Drop casting is used as a basic method to construct 3D-printed electrochemical sensors or biosensors. Janegitz and Muñoz et al. used drop casting technique to modify enzyme on the 3D-printed electrode for the construction of biosensor platform [26, 28]. Physical adsorption by immersing an activated 3D-printed electrode into the target-containing solution is another common method to prepare an enzyme-based biosensor. Our group has utilized the method to construct a direct electron transfer enzyme-based biosensor for the detection of hydrogen peroxide [29]. As proved by our previous work, the electrochemically activated nanocarbon electrode possesses carboxyl active groups [24]. Hence, it is possible to modify the enzyme on the 3D-printed nanocarbon electrode by covalent reaction between carboxyl and amino group in order to obtain a highly stable biosensor.

In this context, the combination of DMF and electrochemical methods was used for the activation of an as-printed 3D nanocarbon electrode. Then, a glucose oxidase-modified 3D-printed nanocarbon electrode was first synthesized by the covalent method using *N*-(3-dimethylaminopropyl)-*N*′-ethylcarbodiimide hydrochloride (EDC) and *N*-hydroxysuccinimide (NHS) as carboxyl-activated reagents. The prepared biosensor platform can be used for the detection of hydrogen peroxide and glucose by chronoamperometry. It shows excellent stability for the sensing of hydrogen peroxide (H_2O_2) and glucose, and opens the door for the covalent modification of 3D-printed electrodes in other fields of electrochemistry.

Experimental section

Materials and reagents

Commercially available Carbon Black 3D raw material filaments composed of graphene and PLA were obtained from Graphene Supermarket (New York, USA). Glucose, glucose oxidase (GOx), acetone, H_2O_2 solution, EDC, NHS, and DMF were purchased from Sigma-Aldrich (St. Louis, MO, USA). Apple cider with 4.5% ethanol was purchased from a grocery store (Brno, Czech Republic). All the solutions for electrochemical analysis were prepared in pH 7.2 phosphate-buffered saline (PBS). All other reagents were at least analytical grade and provided by Sigma-Aldrich. All experiments were carried out at our laboratory's ambient temperature.

Instruments

3D-printed nanocarbon electrodes were printed by FDM technique using a Prusa i3 MK3 3D-printer (Prusa Research, Czech Republic). Electrochemical experiments were carried out by methods of chronoamperometry and cyclic voltammetry (CV) on an Autolab PGSTAT 204 potentiostat (Metrohm, Switzerland). Scanning electron microscopy (SEM) was performed on a Verios 460 L (FEI, USA) to characterize surface morphologies of electrodes. X-ray photoelectron spectroscopy (XPS) was performed to detect the chemical bonds and surface element composition on an AXIS Supra instrument (Kratos Analytical, UK) using a monochromatic Al Kα (1486.7 eV) and X-ray excitation source with 225 W power.

Preparation and activation of 3D-printed nanocarbon electrode

Firstly, the 3D-printed electrode prototype (6 mm diameter, 0.5 mm thickness) was designed by computer using Autodesk Fusion 360 software. Then, 12 electrodes were printed using the Prusa i3 MK3 printer at the same time with 230 °C nozzle temperature and 60 °C bed temperature. Then, these as-printed 3D nanocarbon electrodes were activated by DMF immersion and electrochemical treatment according to our reported method with slight modification; the activated electrode is named DMF-EC [24]. Specifically, as shown in Fig. 1, 3D-printed electrodes were activated in DMF solution for 3 h in order to remove the insulating PLA polymer and expose the conductive graphene nanofiber. These activated electrodes were further washed with acetone and ethanol to remove surface PLA, and then dried in the oven at 50 °C for the following electrochemical activation. Next, the electrochemical condition of 2.5 V potential for 300 s in PBS was chosen for further executing the electrochemical activation.

Covalent modification for the construction of a biosensor platform

After the activation procedure, the nanocarbon electrode was firstly reacted with EDC (0.4 mM) and NHS (0.4 mM) solution for 2 h to activate the surface carboxyl, and then washed with PBS. Afterward, the activated electrode was incubated in

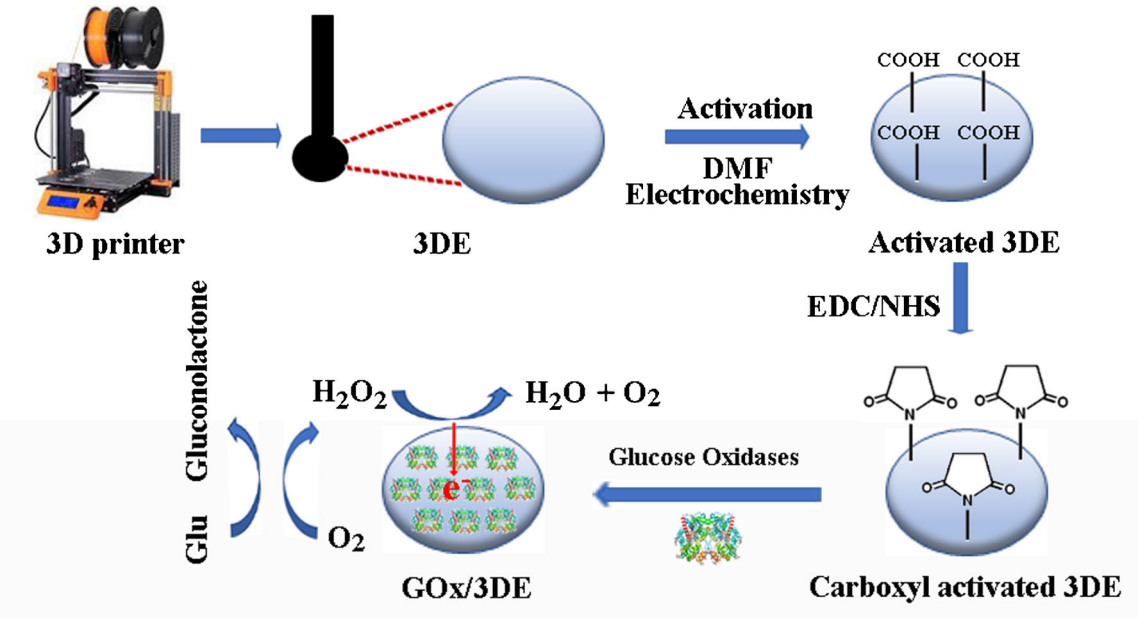

Fig. 1 Scheme for the construction of covalent modified glucose oxidase-based 3D-printed nanocarbon electrode and the corresponding mechanism for the detection of H_2O_2 and glucose

5 mg/mL GOx solution to carry out the condensation reaction with stirring at 7 °C for 24 h followed by washing in the PBS for several times to remove unreacted GOx (Fig. 1). The GOx-modified 3D-printed electrode, named as GOx/3DE, was stored in PBS at 4 °C for next use.

Electrochemical measurements

The main biosensing mechanism of our device is the use of glucose oxidase as substrate (glucose), converted selectively to gluconic acid and hydrogen peroxide, which is detected on the electrode surface. Therefore, the electrochemical property and the determination of hydrogen peroxide were first studied by CV and chronoamperometry, and the glucose was detected by chronoamperometry. Electrochemical measurements were carried out using GOx/3DE as working electrodes; a platinum wire and an Ag/AgCl electrode were chosen as counter and reference electrodes, respectively. CVs were performed at a scan rate of 25 mV s^{-1} from 0 to 1.0 V in the PBS pH 7.2 solution. Chronoamperometric measurements were carried out with a constant potential of 0.85 V in 5 mL PBS pH 7.2 solution. 2.5 μL of 100 mM H_2O_2 solution was added during

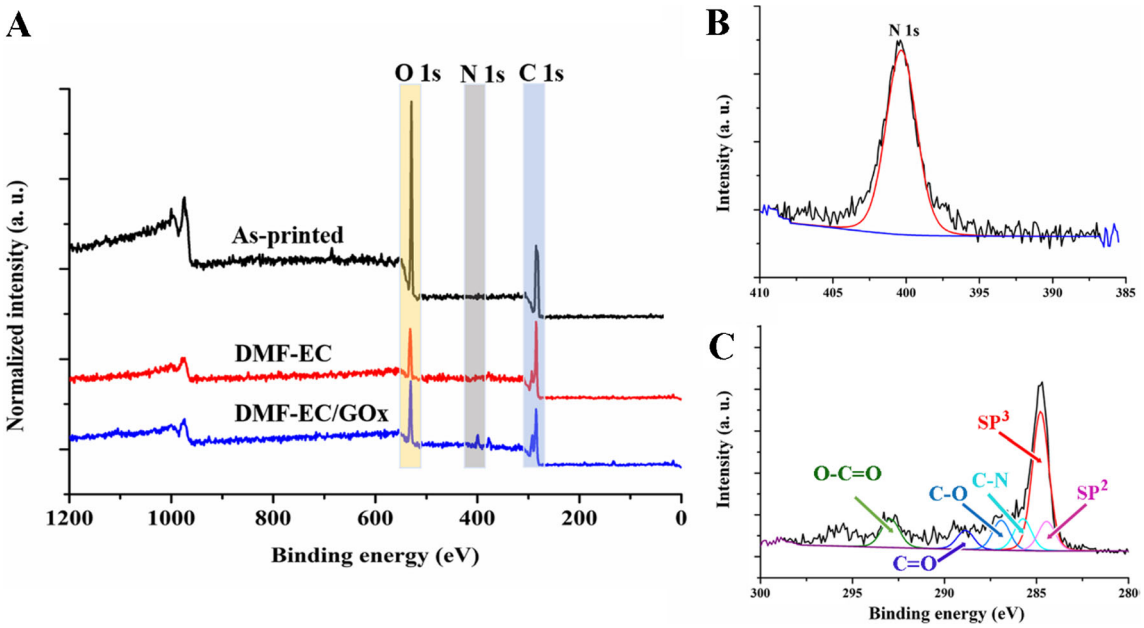

Fig. 2 (A) XPS survey of different electrodes: As-printed, DMF-EC, and GOx/3DE. High-resolution XPS spectra of (B) N 1 s and (C) C 1 s of GOx/3DE

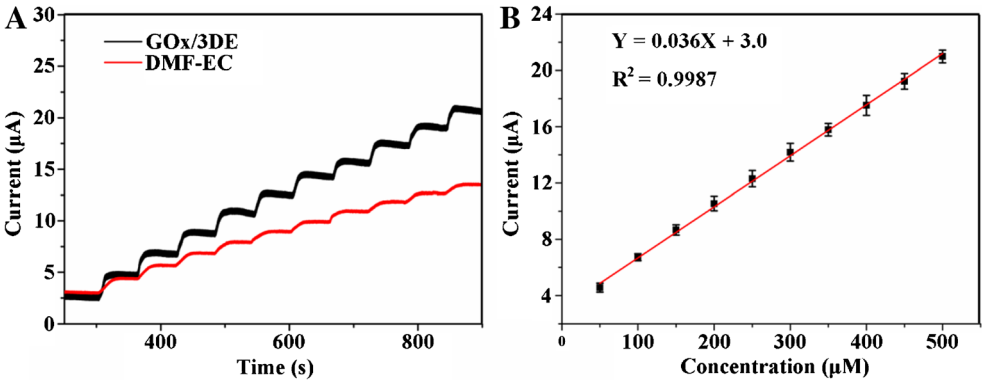

Fig. 3 (A) Chronoamperometry responses under successive additions of 50 μM H_2O_2 in PBS (pH 7.2) with an applied potential of 0.85 V vs Ag/AgCl. (B) Linear plot of calibration curve of current response versus H_2O_2 concentration of GOx/3DE biosensor

each 60 s under slight stirring to obtain H_2O_2 concentrations in the range of 50–500 μM. Aliquots of 2.5 μL of 1000 mM glucose were added in the working solution to get the glucose concentrations in the range of 0.5–10 mM. The repeatability for H_2O_2 and glucose detection on the GOx/3DE biosensor using chronoamperometry was under the concentration of 50 μM and 500 μM, respectively.

Results and discussion

Characterizations of 3D-printed and enzyme-modified nanocarbon electrodes

The final GOx-modified 3D-printed biosensor was prepared by the covalent modification of GOx on the activated nanocarbon electrode using EDC and NHS reagents [30, 31]. Then, XPS measurements were first used to analyze the chemical compositions and structures of different synthetic nanocarbon electrodes. Figure 2A shows the survey spectra of as-printed, DMF-EC, and GOx/3DE electrodes. Table S1 presents the detailed elemental composition of these prepared nanocarbon electrodes; respectively, the compositions of C, O, and N of GOx/3DE electrodes are 78.52%, 16.63%, and 4.85%. From the survey spectra and elemental table, C and O peaks at ~284.2 and 253.6 eV, respectively, are the two main elements presenting in as-printed, DMF-EC, and GOx/3DE electrodes. N 1 s peak at ~400.4 eV is observed on the survey spectra of GOx/3DE, which indicates GOx is modified on the surface of activated electrode. High-resolution XPS was further used to obtain information of nitrogen and carbon functional groups on the GOx/3DE surface (Fig. 2B and Fig. 2C). N 1 s at ~400.4 eV corresponds to the peak of -O=C-N- from the covalent reaction between amino and carboxyl groups. C 1 s spectrum of GOx/3DE displays its three components of C-C/C-H (sp^3, ~284.6 eV), C-O (~286.9 eV), and C=O (~288.9 eV) from PLA polymer, and three components of C=C (sp^2, ~284.3 eV), C-N (~285.7 eV), and O-C=O (~292.7 eV) from graphene and GOx. C 1 s spectra of different electrodes (Fig. S1) show that the C-O and C=O groups from the PLA polymer decreased from as-printed electrode to activated electrode; the C-N group appeared after the modification of GOx on the activated electrode. Detailed information of nitrogen and carbon functional groups also indicates that GOx has been modified on the surface of the DMF-EC.

In addition, the surface morphologies of as-printed, DMF-EC, and GOx/3DE were characterized by SEM. As shown in Fig. S2A, the surface of the as-printed electrode is covered by non-conducting PLA polymer. After activation by the methods of DMF and EC, smooth graphene nanofibers are exposed on the electrode surface and the surface area can be increased after the activation procedure (Fig. S2B). Then, the surface morphology of graphene is changed from smooth to rough due to the modification of GOx on the surface of the graphene fibers (Fig. S2C). These results also indicate the successful synthesis of GOx/3DE.

Determination of hydrogen peroxide

Optimization of glucose oxidase concentration (Fig. S3A and Fig. S3B) and detection condition of glucose (Fig. S3C and Fig. S3D) can be found in the support information. Finally, 5 mg mL^{-1} GOx-modified 3D-printed biosensor and PBS of pH 7.2 were chosen for the sensor of H_2O_2 and glucose.

Table 1 Analytical performance of GOx/3DE biosensor

Biosensor	Analytes	Analytical Range	Linearity	LOD	LOQ	RSD
GOx/3DE	H_2O_2	50–500 μM	0.9987	2.97 μM	8.91 μM	7.0%
	Glucose	0.5–10 mM	0.9979	158 μM	473 μM	1.4%

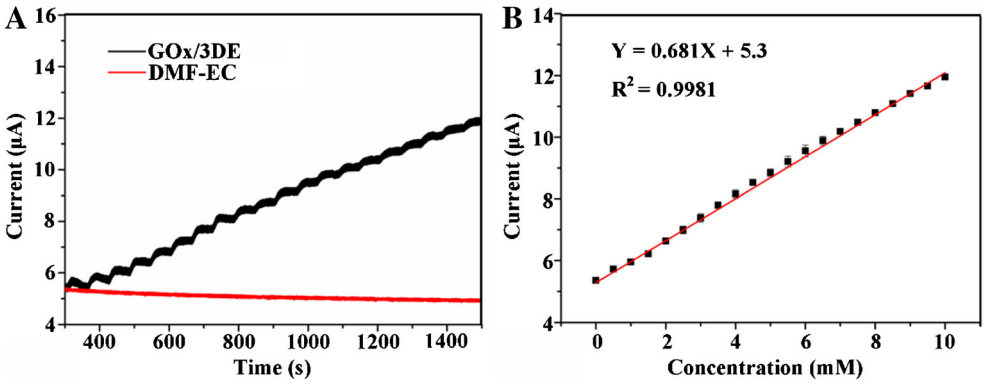

Fig. 4 (A) Chronoamperometry responses under successive additions of 500 μM glucose in PBS (pH 7.2) with an applied potential of 0.85 V vs Ag/AgCl for the DMF-EC (red line) and GOx/3DE (black line). (B) Linear plot of calibration curve of current response versus glucose concentration of GOx/3DE biosensor

H_2O_2 is considered a significant component in life factors [32, 33]. The main biosensing mechanism of our device uses glucose oxidase as substrate (glucose) converted selectively to gluconic acid and hydrogen peroxide, which is detected on the electrode surface. Therefore, the electrochemical property of GOx/3DE for the oxidation of H_2O_2 was first studied by CV. Specifically, CVs of GOx/3DE biosensor in PBS pH 7.2 containing different concentrations of H_2O_2 are displayed in Fig. S4A. The CV results indicate that electro-oxidation of H_2O_2 appears at potential greater than 0.7 V on GOx/3DE biosensor; i.e., current responsiveness increases with the increase of H_2O_2 concentration. The mechanism for the detection of H_2O_2 can be explained as the oxidizing reaction Eq. (1) and the corresponding scheme shown in Fig. 1. As shown in Fig. S4B, the calibration curve of different H_2O_2 concentrations versus current responsiveness of GOx/3DE is obtained at the potential of 0.85 V, which shows good linear with the H_2O_2 concentration range of 1–10 mM (R^2 = 0.9947).

$$H_2O_2 - 2e^- \rightarrow H_2O + O_2 \quad (1)$$

From the CV results, current responsiveness increases linearly with the increase of H_2O_2 concentration at the oxidation potential of 0.85 V. Hence, the 0.85 V potential was further chosen for the detection of H_2O_2 using chronoamperometry on electrodes of DMF-EC and GOx/3DE. As shown in Fig. 3A, both 3D-printed nanocarbon electrodes of DMF-EC and GOx/3DE show very good current responsiveness after each H_2O_2 addition. These results demonstrate that both DMF-EC and GOx/3DE biosensors are good platforms for the oxidation of H_2O_2. The detection of H_2O_2 on the GOx/3DE biosensor is not affected by the enzyme activity of GOx. This can be ascribed to graphene being an excellent electron medium that can increase electron transfer on the electrode surface [34]. However, the GOx/3DE biosensor shows slightly stronger current responsiveness than DMF-EC, which may be ascribed to the increase of affinity between GOx/3DE and H_2O_2 analyte [35]. Figure 3B shows straight linearity (R^2 = 0.9987) between H_2O_2 concentration and current responsiveness using the chronoamperometry on the GOx/3DE-based biosensor. The limit of detection (LOD) and limit of quantitation (LOQ) for the detection of H_2O_2 on GOx/3DE are 2.97 μM and 8.91 μM, respectively. The values of LOD and lineal range can compare with other reported H_2O_2 biosensor systems (Table S2). In addition, the biosensor displays good repeatability (RSD = 7.0%) for independent assays on three different GOx/3DE. More details for these analytical parameters can be found in Table 1.

Determination of glucose

Glucose is considered an important biomarker for the detection of diabetes and is widely used as a food additive to control

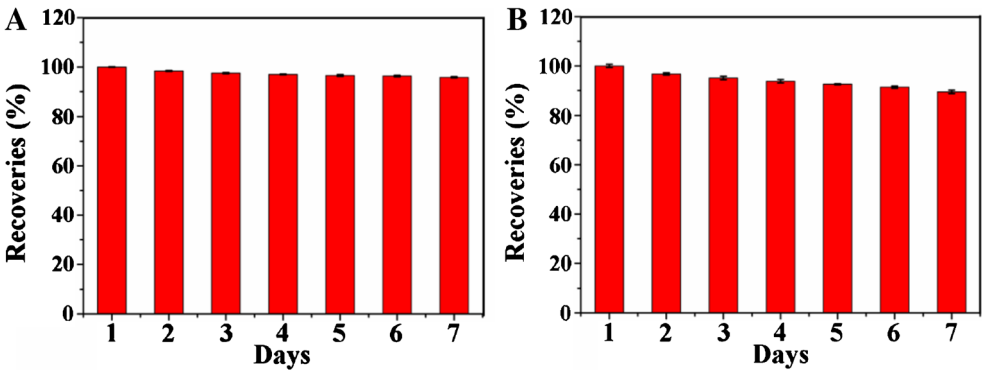

Fig. 5 Long-term stability experiments of chronoamperometric responses on GOx/3DE for 50 μM H_2O_2(A) and 500 μM glucose (B) in pH 7.2 PBS

taste [36–39]. As reported, glucose can react with GOx and produce H_2O_2 following reaction (2); then, H_2O_2 can be detected by the GOx/3DE biosensor [40–43].

$$\text{Glucose} + O_2 \xrightarrow{GOx} \text{Gluconic acid} + H_2O_2 \quad (2)$$

Based on the mechanism and the importance of glucose sensing, the GOx/3DE biosensor was further used for the indirect determination of glucose using chronoamperometric measurements. As shown from Fig. 4A, a good gradient of current responsiveness appeared after each addition of glucose. 3D-printed electrode of DMF-EC without GOx was chosen to execute the control experiment. However, no increased current signal was observed on the DMF-EC biosensor. These results indicate that the current response for the detection of glucose comes from the indirect detection of H_2O_2. It also shows straight linearity (R^2 = 0.9979) for the detection of glucose, with concentration ranging from 0.5 to 10 mM based on the GOx/3DE biosensor (Fig. 4B and Table 1). The LOD and LOQ for the detection of glucose on the GOx/3DE biosensor are 158 μM and 473 μM, respectively. The biosensor shows good repeatability for the detection of glucose with RSD about 1.4% by three independent experiments.

The selectivity and real sample analysis of GOx/3DE

The sugar content of apple cider has an important effect on its sweetness, overall taste, and nutritional value [44]. Hence, the detection of individual sugars, such as glucose, in a sample of apple cider is significant. Hence, the biosensor was finally chosen for the determination of glucose in apple cider. As shown in Fig. S5, 1% apple cider shows significant current responsiveness and the content of glucose in apple cider is calculated as 4.5 ± 0.3 g/L. The interference of 1% ethanol shows a slight current signal on the GOx/3DE sensor, which can be considered negligible. Hence, the prepared sensor has good selectivity for the detection of glucose in apple cider. In addition, concentrations of 500 μM, 2 mM, and 4 mM glucose were prepared by 4.5% ethanol PBS. The recoveries were calculated based on the linear equation between current response (y, μA) and glucose concentration (x, mM): y = 0.681 x + 5.3, which was described in the part of determination of glucose. The recoveries for these three standard solutions were calculated as 97.6% ± 1.0%, 98.5% ± 1.4%, and 96.3% ± 1.5%, respectively. Every measurement was detected three times on the GOx/3DE sensor. These results indicate that the GOx/3DE sensor can be used for the detection of glucose in practical samples.

The long-term stability of GOx/3DE biosensor

As can be seen in Fig. 5, the long-term stability experiments on GOx/3DE for the chronoamperometric responses of 50 μM H_2O_2 and 500 μM glucose up to 7 days were studied. The detection of H_2O_2 on GOx/3DE can retain about 96% initial current responsiveness after 7 days. The high stability for the detection of H_2O_2 mainly ascribes to the non-enzymatic activity dependent. After 7 days, the percentage of recovery for the detection of glucose decreases to about 90% of initial current responsiveness. The result can be ascribed to the slight loss of the enzyme activity of GOx. The GOx/3DE-based biosensor exhibits comparable and even higher stability for determination of glucose compared to previous reported works (Table S3), and the common immobilized reagent nafion is not required in this work. These results indicate that covalent immobilization of the enzyme on the electrode can improve the sensor stability more than simply physical adsorption.

Conclusion

In this work, we activated as-printed 3D nanocarbon electrodes by the combined methods of chemical and electrochemical treatments, and then constructed a GOx-modified 3D-printed nanocarbon electrode by covalent reaction using activated reagents of EDC and NHS. The enzyme-immobilized 3D-printed nanocarbon electrode shows efficient abilities for the detection of H_2O_2 and glucose. The prepared GOx/3DE biosensor can maintain enzyme activity and exhibits excellent stability for the determination of H_2O_2 and glucose, this can compare with other reported biosensors. The GOx/3DE further shows potency for practical application by the detection of glucose in apple cider. We can foresee the using of 3D printing technique for constructing of various portable electrochemical glucose sensor using in practical samples. This work opens new avenues not only for the covalent immobilization of enzymes on 3D-printed nanocarbon electrodes for (bio)sensing but also other fields of electrochemistry including batteries, energy storage, and catalysis.

Supplementary Information The online version contains supplementary material available at https://doi.org/10.1007/s00604-021-05006-6.

Acknowledgements M.P. was supported by the Grant Agency of the Czech Republic (GACR EXPRO: 19-26896X). L.W. thanks CzechNanoLab Research Infrastructure for the support of material characterizations (ID LM2018110, MEYS CR, 2020-2022). We thank the S.N. for performing the SEM and XPS characterizations, and W.G. for the discussion of scientific questions.

Author contribution Lujun Wang: conceptualization, methodology, data curation, investigation, writing—original draft, writing—review & editing. Martin Pumera: conceptualization, funding acquisition, project administration, resources, supervision, writing—review & editing.

Declarations

Conflict of interest The authors declare no competing interests.

References

1. Choong YYC, Tan H, Patel DC, Choong WTN, Chen C, Low HY, Tan M, Patel CD, Chua CK (2020) The global rise of 3d printing during the COVID-19 pandemic. Nat Rev Mater 5:637–639
2. Ngo TD, Kashani A, Imbalzano G, Nguyen KTQ, Hui D (2018) Additive manufacturing (3D printing): a review of materials, methods, applications and challenges. Composites Part B 143: 172–196
3. Wang L, Pumera M (2021) Recent advances of 3d printing in analytical chemistry: focus on microfluidic, separation, and extraction devices. TrAC Trends Anal Chem 135:116151
4. Browne MP, Redondo E, Pumera M (2020) 3D printing for electrochemical energy applications. Chem Rev 120:2783–2810
5. Muñoz J, Pumera M (2020) 3D-printed biosensors for electrochemical and optical applications. TrAC Trends Anal Chem 128:115933
6. Ambrosi A, Pumera M (2018) Sel-containedpolymer/metal 3D printed electrochemical platform for tailored water splitting. Adv Funct Mater 28:1700655
7. Ng S, Iffelsberger C, Sofer Z, Pumera M (2020) Tunable room-temperature synthesis of ReS_2 bicatalyst on 3D- and 2D-printed electrodes for photo- and electrochemical energy applications. Adv Funct Mater 30:1910193
8. Symes MD, Kitson PJ, Yan J, Richmond CJ, Cooper GJ, Bowman RW, Vilbrandt T, Cronin L (2012) Integrated 3D-printed reactionware for chemical synthesis and analysis. Nat Chem 4: 349–354
9. Browne MP, Urbanova V, Plutnar J, Novotný F, Pumera M (2020) Inherent impurities in 3D-printed electrodes are responsible for catalysis towards water splitting. J Mater Chem A 8:1120–1126
10. Lee JY, An J, Chua CK (2017) Fundamentals and applications of 3D printing for novel materials. Appl Mater Today 7:120–133
11. Valot L, Martinez J, Mehdi A, Subra G (2019) Chemical insights into bioinks for 3D printing. Chem Soc Rev 48:4049–4086
12. Helú MAB, Liu L (2021) Fused deposition modeling (FDM) based 3D printing of microelectrodes and multi-electrode probes. Electrochim Acta 365:137279
13. Manzanares Palenzuela CL, Novotny F, Krupicka P, Sofer Z, Pumera M (2018) 3D-printedgraphene/polylactic acid electrodes promise high sensitivity in electroanalysis. Anal Chem 90:5753–5757
14. Bin Hamzah HH, Keattch O, Covill D, Patel BA (2018) The effects of printing orientation on the electrochemical behaviour of 3D printed acrylonitrile butadiene styrene (ABS)/carbon black electrodes. Sc Rep 8:1–8
15. Katic V, Dos Santos PL, Dos Santos MF, Pires BM, Loureiro HC, Lima AP, Queiroz JCM, Landers R, Munoz RAA, Bonacin JA (2019) 3D printed graphene electrodes modified with prussian blue: emerging electrochemical sensing platform for peroxide detection. ACS Appl Mater Interfaces 11:35068–35078
16. Munoz J, Redondo E, Pumera M (2021) Bistable (supra)molecular switches on 3D-printed responsive interfaces with electrical readout. ACS Appl Mater Interfaces 13:12649–12655
17. Richter EM, Rocha DP, Cardoso RM, Keefe EM, Foster CW, Munoz RAA, Banks CE (2019) Complete additively manufactured (3D-printed) electrochemical sensing platform. Anal Chem 91: 12844–12851
18. Akshay Kumar KP, Ghosh K, Alduhaish O, Pumera M (2021) Dip-coating of mxene and transition metal dichalcogenides on 3D-printed nanocarbon electrodes for the hydrogen evolution reaction. Electrochem Commun 122:106890
19. Ng S, Iffelsberger C, Michalicka J, Pumera M (2021) Atomic layer deposition of electrocatalytic insulator Al_2O_3 on three-dimensional printed nanocarbons. ACS Nano 15:686–697
20. Elbadawi M, Ong JJ, Pollard TD, Gaisford S, Basit AW (2021) Additive manufacturable materials for electrochemical biosensor electrodes. Adv Funct Mater 31:2006407
21. Gusmão R, Browne MP, Sofer Z, Pumera M (2019) The capacitance and electron transfer of 3D-printed graphene electrodes are dramatically influenced by the type of solvent used for pre-treatment. Electrochem Commun 102:83–88
22. Kalinke C, Neumsteir NV, Roberto de Oliveira P, Janegitz BC, Bonacin JA (2020) Sensing of L-methionine in biological samples through fully 3D-printed electrodes. Anal Chim Acta 1142:135–142
23. Tan C, Nasir MZM, Ambrosi A, Pumera M (2017) 3D printed electrodes for detection of nitroaromatic explosives and nerve agents. Anal Chem 89:8995–9001
24. Browne MP, Novotny F, Sofer Z, Pumera M (2018) 3D printed graphene electrodes' electrochemical activation. ACS Appl Mater Interfaces 10:40294–40301
25. Cardoso RM, Castro SVF, Silva MNT, Lima AP, Santana MHP, Nossol E, Silva RAB, Richter EM, Paixão TRLC, Muñoz RAA (2019) 3D-printed flexible device combining sampling and detection of explosives. Sensors Actuators B Chem 292:308–313
26. Cardoso RM, Silva PRL, Lima AP, Rocha DP, Oliveira TC, do Prado TM, Fava EL, Fatibello-Filho O, Richter EM, Muñoz RAA (2020) 3D-printedgraphene/polylactic acid electrode for bioanalysis: biosensing of glucose and simultaneous determination of uric acid and nitrite in biological fluids. Sensors Actuators B Chem 307:127621
27. Manzanares-Palenzuela CL, Hermanova S, Sofer Z, Pumera M (2019) Proteinase-sculptured 3D-printed graphene/polylactic acid electrodes as potential biosensing platforms: towards enzymatic modeling of 3D-printed structures. Nanoscale 11:12124–12131
28. Silva V, Fernandes-Junior WS, Rocha DP, Stefano JS, Munoz RAA, Bonacin JA, Janegitz BC (2020) 3D-printed reduced graphene oxide/polylactic acid electrodes: a new prototyped platform for sensing and biosensing applications. Biosens Bioelectron 170:112684
29. Lopez Marzo AM, Mayorga-Martinez CC, Pumera M (2020) 3D-printed graphene direct electron transfer enzyme biosensors. Biosens Bioelectron 151:111980
30. Luo Q, Zhong Z, Zheng Y, Gao D, Xia Z, Wang L (2021) Preparation and evaluation of a poly(*n*-isopropylacrylamide) derived graphene quantum dots based hydrophilic interaction and reversed-phase mixed-mode stationary phase for complex sample analysis. Talanta 224:121869
31. Supraja P, Tripathy S, Krishna Vanjari SR, Singh V, Singh SG (2019) Electrospun tin (IV) oxide nanofiber based electrochemical sensor for ultra-sensitive and selective detection of atrazine in water at trace levels. Biosens Bioelectron 141:111441
32. Kogularasu S, Govindasamy M, Chen SM, Lin SH, Akilarasan M, Mani V (2018) A novel synthesis of non-aggregated spinel nickel ferrite nanosheets for developing non-enzymatic reactive oxygen species sensor in biological samples. Sensors Actuators B Chem 266:655–663
33. Sakthivel K, Govindasamy M, Chen SM, Muthumariappan A, Mani V, Selvaraj S (2017) 3D graphene oxide-cobalt oxide polyhedrons for highly sensitive non-enzymatic electrochemical determination of hydrogen peroxide. Sensors Actuators B Chem 253: 773–783
34. Lawal AT (2018) Progress in utilisation of graphene for electrochemical biosensors. Biosens Bioelectron 106:149–178
35. Liu Y, Wang M, Zhao F, Xu Z, Dong S (2005) The direct electron transfer of glucose oxidase and glucose biosensor based on carbon nanotubes/chitosan matrix. Biosens Bioelectron 21:984–988
36. Cai Y, Liang B, Chen S, Zhu Q, Tu T, Wu K, Cao Q, Fang L, Liang X, Ye X (2020)One-step modification of nano-polyaniline/glucose oxidase on double-side printed flexible electrode for continuous

glucose monitoring: characterization, cytotoxicity evaluation and in vivo experiment. Biosens Bioelectron 165:112408
37. Guzsvány V, Anojčić J, Vajdle O, Radulović E, Madarász D, Kónya Z, Kalcher K (2019) Amperometric determination of glucose in white grape and in tablets as ingredient by screen-printed electrode modified with glucose oxidase and composite of platinum and multiwalled carbon nanotubes. Food Anal Methods 12:570–580
38. Zhang Z, Chen Z, Cheng F, Zhang Y, Chen L (2017) Highly sensitive on-site detection of glucose in human urine with naked eye based on enzymatic-like reaction mediated etching of gold nanorods. Biosens Bioelectron 89:932–936
39. Akilarasan M, Kogularasu S, Chen SM, Chen TW, Govidasamy M, Lou BS (2018) Effects of annealing temperature on crystal structure and glucose sensing properties of cuprous oxide. Sensors Actuators B Chem 266:655–663
40. Ikeda M, Tanida T, Yoshii T, Kurotani K, Onogi S, Urayama K, Hamachi I (2014) Installing logic-gate responses to a variety of biological substances in supramolecular hydrogel–enzyme hybrids. Nat Chem 6:511–518
41. Mani V, Devadas B, Chen SM (2013) Direct electrochemistry of glucose oxidase at electrochemically reduced graphene oxide-multiwalled carbon nanotubes hybrid material modified electrode for glucose biosensor. Biosens Bioelectron 41:309–315
42. Sanchez-Calvo A, Costa-Garcia A, Blanco-Lopez MC (2020)Paper-based electrodes modified with cobalt phthalocyanine colloid for the determination of hydrogen peroxide and glucose. Analyst 145: 2716–2724
43. Salimi A, Compton RG, Hallaj R (2004) Glucose biosensor prepared by glucose oxidase encapsulated sol-gel and carbon-nanotube-modified basal plane pyrolytic graphite electrode. Anal Biochem 333:49–56
44. Hu G, Liu H, Zhu Y, Hernandez M, Koutchma T, Shao S (2018) Suppression of the formation of furan by antioxidants during UV-C light treatment of sugar solutions and apple cider. Food Chem 269: 342–346